Krill-eye : Superposition Compound Eye
for Wide-Angle Imaging via GRIN Lenses

Shinsaku Hiura[*]   Ankit Mohan   Ramesh Raskar

Camera Culture Group, MIT Media Lab

http://cameraculture.info

Abstract

We propose a novel wide angle imaging system inspired by compound eyes of animals. Instead of using a single lens, well compensated for aberration, we used a number of simple lenses to form a compound eye which produces practically distortion-free, uniform images with angular variation. The images formed by the multiple lenses are superposed on a single surface for increased light efficiency. We use GRIN (gradient refractive index) lenses to create sharply focused images without the artifacts seen when using reflection based methods for X-ray astronomy. We show the theoretical constraints for forming a blur-free image on the image sensor, and derive a continuum between 1 : 1 flat optics for document scanners and curved sensors focused at infinity. Finally, we show a practical application of the proposed optics in a beacon to measure the relative rotation angle between the light source and the camera with ID information.

1. Introduction

In this paper, we propose a novel wide angle imaging system which realizes practically uniform image quality for any angle of view without distortion. For more than a century, lens designers and manufacturers have struggled to balance image quality and cost for wide angle lenses [15]. Most current wide angle lens designs are simply adapted from normal standard field of view lens designs, making it extremely hard to minimize the distortions and obtain uniform images. On the other hand, many animals, specially insects, use compound eyes made up of multiple simple lenses to achieve a vision system with extremely wide field of view. We explore this somewhat unusual optical design for building a general purpose wide angle imaging system.

Compound eyes can be classified into two categories, *apposition* and *superposition* [17]. Apposition is common among most diurnal insects and crustaceans (e.g. bees and crabs). However, the amount of incoming light on a photo receptor is limited because the size of the aperture of each ommatidium (one optical unit of compound eye) is very small [10]. Diffraction effects greatly limit the angular sensitivity of each ommatidium, thus limiting the overall angular resolution. The maximum resolving power of a lens is expressed by Dawes' limit [1] $R \approx 116/D$, where D is the diameter of the lens in millimeters and R is the re-
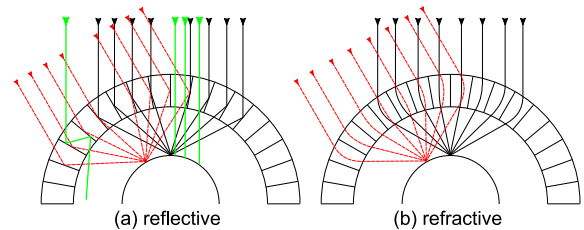

Figure 1. Principle of superposition compound eyes. (a) Reflecting superposition compound eye found in decapod shrimps and lobsters (b) Refracting superposition compound eye of moths and krill.
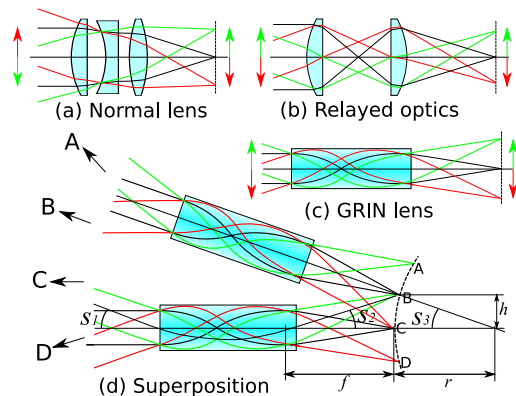

Figure 2. Superposition by GRIN lenses. Unlike a normal lens (a) which forms an image flipped upside-down, image by certain length of GRIN rod lens (c) is upright as a Keplerian telescope, (b). Therefore the spherical array of GRIN lenses (d) produces superposed and focused images on a sphere.
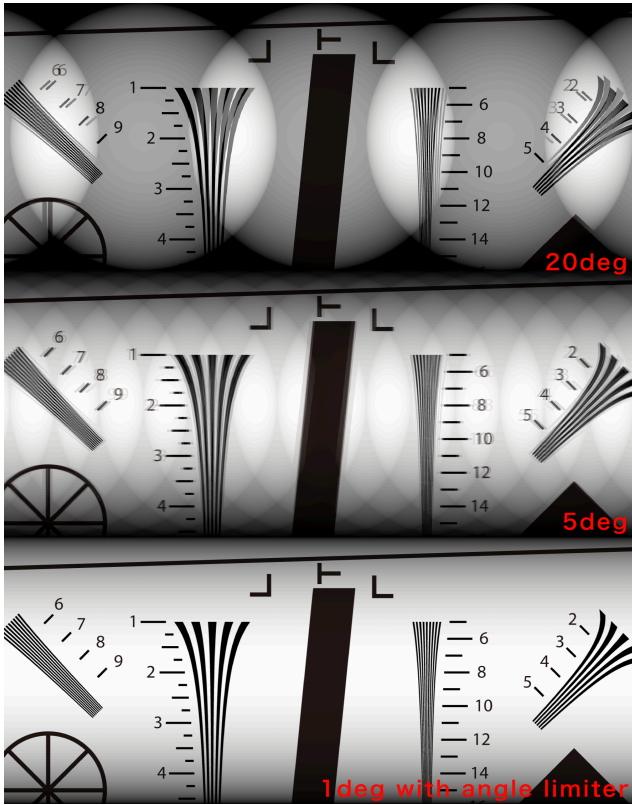
---
[*]now at Osaka University

Figure 3. Computationally generated images to show the image quality of Krill-eye. We simulate the approximation error of superposition constraint and vignetting effect. Dense arrangement of ommatidia improves image quality, and the angle limiter (shade) reduces the effects of misalignment error. See supplemental materials for all simulated images in high resolution.

solving power in arcseconds. Therefore, each lens should be shared by multiple pixels to acquire sufficient light and angular resolution.

Some animals living in dim environments use a superposition compound eye to gather more incoming light onto a photo receptor through multiple optical elements. As shown in Figure 1, two types of superposition compound eyes are known to exist. The reflecting superposed compound eye found in decapod shrimps and lobsters collects light using an array of mirrors arranged in a sphere. This design has a clear advantage for applications in which refracting optical elements are not possible, such as X-ray imaging [5, 2]. However, this reflection based design results in artifacts that degrade the image quality. As shown in Figure 1(a), an incoming light ray must reflect only once (or twice in the 3-D case), or it will hit the wrong point on the photo receptor array. Additionally, the resolution of the image is limited by the pitch of the micro mirror elements because each ommatidium has no effect on focusing. On the other hand, the refracting superposition compound eye (Figure 1(b)) bends

incoming light rays and focuses them on the opposite side of optical axis of each lens element as shown in Figure 2(c). This type of optics found in krill and moths is free of these artifacts. However, these optics have been researched only in biological studies, and not for engineering applications. In this paper, we show theoretical constraints of these optics to form a sharp image as shown in Figure 3 with a practical application to measure the relative rotation angle between a light source and a camera.

1.1. Related work

In computer vision area, several applications make use of extremely wide field of view cameras. They have several advantages for geometric analysis such as epipolar geometry [25] or motion estimation [11], and also useful for the radiometric compensation [22] and tele-presense [20]. Several optical systems for wide field of view imaging have been proposed, such as catadioptric system [27]. Unfortunately, it has no uniformity in either resolution or illumination. We explore a novel animal vision inspired device to achieve uniform imaging in angle.

There are several studies inspired by compound eyes of animals. The work by Duparre et al. [6] is a straight-forward implementation of apposition compound eye to realize a ultra-thin imaging device. As described above, both the resolution and light efficiency are theoretically limited for the apposition compound eye [10], and multiple photo receptors are needed for each lens element in most cases. For example, TOMBO (Thin Observation Module by Bound Optics) [7] uses a miniature lens array on the image sensor. However, this structure is essentially a camera array and extends neither the field of view, nor the resolution.

Superposed compound eyes are also studied as thin optics for imaging. The Gabor superlens [9, 4, 3] is an array of Keplerian telescopes that form upright images on the image sensor for superposition. However, each lens in one optical unit should be shifted to make angular variations, and this naturally it limits the field of view of the system. In other words, the field of view of the system cannot exceed the field of view of each small lens, and it is difficult to make super-wide angle optics with flat photo receptors.

As described above, mirror based superposition compound eyes are used for X-ray imaging. Lobster-ISS [5] is a wide-angle X-ray imaging device for detecting astronomical events such as supernova explosions. LEXID [2] is also a device for X-ray imaging for inspection. However, the image formed by the reflecting superposition eye is degraded by artifacts [23] as shown in Figure 1(a).

1.2. Contributions

We propose a novel design for wide angle imaging, called the 'Krill-eye', inspired by the superposition based animal eyes. Our technical contributions are as follows:

- We obtain two constraints, the **superposition constraint** and the **focusing constraint**, which when satisfied simultaneously result in a sharply focused image on the sensor.

- We derive a continuous relationships between the $1 : 1$ flat imaging system currently used for optical scanners, and the infinity focused animal eye design with a curved image sensor.

- We apply this theory to design and build a prototype, and use it to confirm image quality.

- We present a practical application of the proposed imaging system as a beacon to measure the relative rotation angle between the beacon and the camera.

1.3. Limitations

A wide angle imaging device with a compound eye requires a curved or spherical image sensor. Several recent advances in silicon fabrication make this possible. Dinyari et al. [8] made a curved image sensor with flexible interconnects between tiny silicon chips with photo detectors, and Grayson [12] made it with thinned silicon wafer curved in a pressure chamber. Swain and Mark [26] proposed an optical setup for curved sensors, but their design still uses a lens with a single optical axis.

The resolution of the Krill-eye optics is diffraction limited. If we use a single lens with well compensated aberration, the resolution on the sensor is determined by F-number. By superposition with several lenses, we gain in terms of light efficiency, but not in terms of improved resolution. However, for the wide-angle lenses, the main cause of resolution degradation is not diffraction but aberration resulting from imperfect lens design.

2. Constraints for Superposition

An image formed by a normal convex lens is flipped both vertically and horizontally (Figure 2(a)). We can produce an upright image by focusing the inverted intermediate image to the final sensor using a second lens (relayed optics or Keplerian telescopes) as shown in Figure 2(b). Such a setup is also used for the Gabor Super Lens [9]. Alternatively, a gradient index (GRIN) rod lens (Figure 2(c)) also results in a similar upright image. A GRIN lens array [24] is widely used as the imaging system in many low-cost scanners. Such GRIN lens arrays are limited to $1 : 1$ (life-size) imaging because all lenses are aligned parallel to one another. We propose a novel optical design for an omnidirectional imaging system: multiple GRIN rod lenses, aligned on a circle (or a sphere), with all optical axes intersecting at one point (Figure 2(d)). Such a setup focuses an object at infinity onto a spherical sensor.
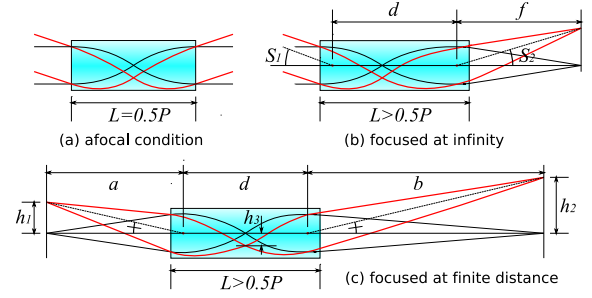
Figure 4. Imaging property of a GRIN rod lens. (a) afocal condition ($f = \infty$) with pitch (length) $P = 0.5$ GRIN lens. (b) a GRIN rod working as converging lens focused at infinity with focal length f. (c) same lens focused at finite distance.

In the general case, two constraints described below must be satisfied simultaneously to result in a sharp image on the sensor.

Superposition Constraint: Light rays from any given point in the world, passing through several GRIN lenses, should be registered at a single point on the image sensor.

Focusing Constraint: Light rays from any given point in the world, passing through a single GRIN lens, should focus at the same point on the image sensor.

2.1. Gradient Refractive Index Lens

Unlike traditional lenses, a GRIN lens has a non-uniform index of refraction. The refractive index is symmetric about the optical axis; highest at the optical axis, and decreasing as a function of the distance r from the optical axis. A typical distribution of the refractive index n_r is

$$n_r = n_0(1 - \frac{A}{2}r^2), \tag{1}$$

where n_0 is the refractive index on the optical axis, and $\sqrt{A}$ is a constant commonly called the gradient-index constant. For such a distribution, a light ray travels along a sinusoidal path inside the lens.

The function of the GRIN rod lens changes with the physical length of the rod lens L. To parameterize it, a constant $P = 2\pi/\sqrt{A}$ called the pitch number is commonly used. If $L = 0.5P$, a light ray forms just a half period of sinusoid within the lens (Figure 4(a)), and a set of parallel rays entering the lens remain parallel to one another when they exit, but their direction is bent to the opposite side of the optical axis.

The focal length f of the GRIN lens can be calculated as

$$f = \frac{1}{n_0\sqrt{A}\sin(L\sqrt{A})}. \tag{2}$$

The focal length is infinite when the length of the lens is $L = 0.5nP$, where n is a natural number. When $L < 0.5P$, the GRIN lens works as a normal converging lens; when $0.5P < L < 1.0P$, we have negative focal length $f < 0$ which means the image is flipped vertically and horizontally (and not a diverging lens). Just like a traditional convex lens, we can define two principal points on the optical axis (separated by a distance d), such that the two rays towards the principal points have the same angle $S_1 = S_2$ with the optical axis (Figure 4(c)). Additionally, the thin lens law holds for a GRIN lens,

$$\frac{1}{a} + \frac{1}{b} = \frac{1}{|f|}. \tag{3}$$

Since the negative f is used for describing not diverging lens but the upright image formation of GRIN lens, we use $|f|$ instead of f. Moreover, just like a conventional lens, image magnification ratio is given by $M = h_2/h_1 = b/a$ as shown in Figure 4(c).

2.2. Superposition focused at infinity

Consider an object at infinity in the direction B as shown in Figure 2(d). Since this object is on the optical axis of the upper lens, the height of the image of B is $h = r\sin(S_3)$. On the other hand, the angle of the ray through the lower lens S_2 is described as

$$S_2 = tan^{-1}\frac{r\sin(S_3)}{f + r - r\cos(S_3)} \tag{4}$$

because the distance from the lens to the image surface is f (by the *focusing constraint*). Additionally, as described in Section 2.1, the angle S_2 is same as S_1. Obviously, the angle S_1 should be same as S_3 for the object at infinity to register the image from these two lenses (by the *superposition constraint*). If the angle S_3 are sufficiently small, it follows that r is equal to the focal length of GRIN lens f. This result is independent of the small angle between GRIN lenses. In other words, the exact arrangement (span) of the lenses does not matter to the superposition constraint, and the lenses should be only aligned radially around a sphere with a certain radius. The angular registration error $S_3 - S_1$ rapidly converges to zero according to the decreasing S_3 as shown in Fgiure 5(a).

2.3. Superposition focused at finite distance

Consider the case where both the object and the image are a finite distance from the lens (Figure 6(b)). The GRIN lenses are aligned radially around the center of two spherical images. By the *focusing constraint*, the difference in the radius of the two spherical images should satisfy,
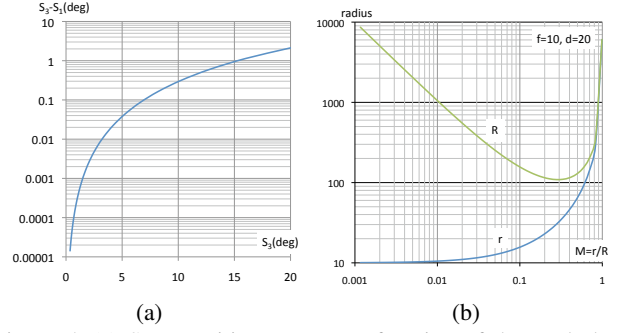
$$|R - r| = a + b + d. \tag{5}$$

Figure 5. (a) Superposition error as a function of the angle between two GRIN lenses calculated by Eq 4. The superposition error $(S_3 - S_1)$ rapidly decreases with smaller S_3. (b) Two radii R and r vary with magnification ratio M under the fixed focal length constraint.

Also a and b satisfy the thin lens law in Eq 3. Simultaneously, image on the spherical surface r should be a similar figure of object surface R, and the magnification ratio M of each lens $M = \frac{b}{a}$ should be same as homothetic ratio of two spheres (by *superpositon constraint*),

$$\frac{b}{a} = \frac{r}{R} = M \tag{6}$$

The two variables a and b can be eliminated by using Eq 3, 5 and 6, giving us

$$M \cdot R = r = \frac{(M + 1)^2|f| + Md}{|M - 1|}. \tag{7}$$

This equation implies that the radii of the spherical surfaces are not arbitrary but given by the magnification ratio M and the focal length f of the GRIN lenses. In other words, we cannot use two arbitrary spheres with fixed focal length lenses. Figure 5(b) shows the relationships between M, r and R for fixed lens parameters $f = 10$ and $d = 20$.

The Eq 7 also corresponds to some known solutions. As shown in Figure 6(a), two image surfaces are flat ($r = R = \infty$) if the magnification ratio is the life size ($M = 1$). This is a case of the optical system used for image scanners and LED based page printers. In this case, the distance between two planes is $4f + d$. The other typical case is the one focused at infinity. Eq 7 indicates that $r = f$ when $M = 0$ as shown in Figure 5(b), and this is a same result shown at Section2.2. Similarly, $\lim_{M\to\infty} R = f$ shows the reverse case of this optics. Therefore, the refractive superposition compound eye has a continuum for magnification ratio as shown in Figure 7. The radius of larger image sphere has a lower limit, for example, $min(R) \approx 108.99$ when $M \approx 0.29$ for the case of $f = 10$ and $d = 20$.

3. Characteristics of the Krill-eye

In this section we discuss the optical characteristics of the Krill-eye imaging system, and compare it with other wide angle imaging designs.

3.1. Aberrations of GRIN lens

Like any optical system, the GRIN lens based designs presented are affected by aberrations that degrade the image quality. In third order optics, we have five Seidel monochromatic aberrations, and two types of chromatic aberrations. These seven aberrations are classified into lateral and transversal aberrations.

Lateral aberrations (distortion, coma aberration, lateral chromatic aberration) of GRIN lens around $L = 0.5P$ are negligible because the design of the GRIN lens itself is symmetric. Lateral aberration caused by the first half of the lens affects to the lateral position of the focus inside the lens, but this shift is automatically compensated by the second half. For example, the height of the internal image for the red wavelength h_3 shown in Figure 4(c) is a little larger than the blue one due to dispersion, but the projection from the internal image h_3 to the last image h_2 compensates the difference of the image size. The same principle works to the other all lateral aberrations, therefore, we do not have to care about the lateral aberrations in our imaging system.

Spherical aberration is very well compensated in GRIN lenses due to the parabolic distribution of the refractive index. Well tuned distribution of refractive index works as an aspherical surface of the usual lens with constant index.

The other **transversal aberrations** (field curvature, astigmatism, transversal chromatic aberration) affect to the
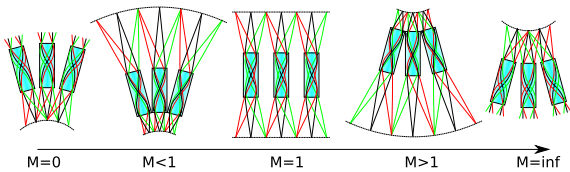
shape of the PSF (point spread function). In particular, transversal chromatic aberration is not compensated at all with single GRIN lens. Fortunately, the impact of transversal aberrations is proportional to the aperture size of the lens (inversely proportional to the F-number). Since the diameter of the GRIN lens determines the aperture size, we can suppress the effect of the transversal aberration by using a thin GRIN lens. For example, flat bed scanners use GRIN lenses with $0.3mm$ diameter.

The effect of **field curvature and astigmatism** increases with the viewing angle, therefore, we can suppress their effect by limiting the field of view of each lens with shades.

Longitudinal chromatic aberration is dominant with relatively thick GRIN lenses. As described above, we can suppress this effect by using a thin GRIN lens, as used for documents scanners.

3.2. Light efficiency and image quality of Krill-eye optics

We can minimize the effect of aberrations by using thin lenses. It means that the effect of the focusing constraint is suppressed and the overall characteristics of the Krill-eye optics is determined by the superposition constraint only.

The other important factor for the image quality of Krill-eye optics is the field of view of each GRIN lens. As shown in Figure 1(b), wider field of view of each lens gathers more light to a single point on the image surface. Therefore, the light efficiency of the Krill-eye optics, which is intuitively similar to the F-number of conventional lens, is determined by the field of view of GRIN lenses. However, the image quality of such massively superposed optics could be worse because the approximation of superposition constraint makes it worse. Therefore, to ensure high image quality, the field of view of each lens should be adequately limited with light barriers such as shades.

The precision of alignment of the optical elements is very important for minimizing artifacts. In our handmade prototype, we have some fluctuation of the lens elements which causes slight misalignment of the image. The alignment of the lenses is simplified because the exact distribution of the lenses on the sphere does not matter to the superposition constraint, and the holes to insert the GRIN lenses should be simply radial which makes them easy to machine.

3.3. Comparison to the other lens designs

In this section we will make clear what is the advantage of our proposed optics by comparing to the other optical designs.

Fish-eye lens (Figure 8(a)) is the most common lens design for wide-angle cameras with an approximately $180°$ field of view. This design has the advantage of a single flat image plane. However, it is very expensive due to the high fabrication cost of lenses with deep spherical surfaces (only
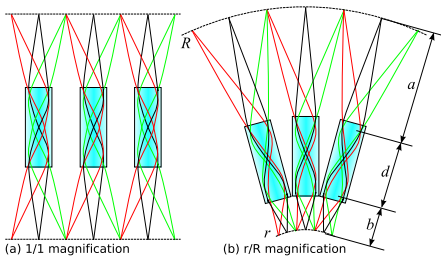
Figure 6. $M = 1/1$ and $M = r/R$ cases of superposition compound optics.

Figure 7. Continuum of magnification on refractive superposition compound eye.

one lens element can be polished at a time). Additionally, the angular resolution of the image plane is not uniform, and it is difficult to cover a field of view larger than 180°. 220° fish-eye lenses are huge, very expensive, and extremely impractical, and a coverage of 360° is impossible. Since the relationship between the image and solid angle is not uniform, these lenses have significant light fall-off in the peripheral region when used for projection. **Catadioptric systems** (mirror-based optics) [27] could be included in this category. Though they have different characteristics for the geometry of projection, they do not have the uniformity for all of resolution, distortion and luminance[13, 21].

Camera arrays (Figure 8(b)) are widely used to acquire spherical photographs and videos. They are also commonly used for omnidirectional projectors in planetariums. This optical system has very high angular resolution with well compensated aberrations, and can cover a large angle of view. However, the system is large because each optical element consist of compound lens system. The registration of images is not easy, and requires high precision optics.

GRIN sphere (Figure 8(c)) is also proposed as a lens without an optical axis, and has potential for use in a wide angle imaging system [16]. It might be very small, and the relationship between the image and the angle is uniform. However, the GRIN ball lens is not easy to manufacture, and it is not available on the market yet. F-number of the lens is directly determined by the diameter of the lens, so the compensation of the all transversal aberration is not easy (there

is no lateral aberration because it has no optical axis). Additionally, it does not cover the whole field of view.

In contrast, the imaging system we present in this paper called the **Krill-eye** (Figure 8(d)) has a single image surface shared with several lens elements. It covers the whole field of view, and the resolution is uniform. The cost of the GRIN rod lenses is now very cheap due to advances in optical fiber manufacturing. Arrays of GRIN rod lenses are now widely used for entry-level document scanners under $100.

4. Evaluation and Application of Krill-eye Optics

In this section, we show an application of our optics for the measurement of the relative rotation angle between a light source and the camera as Bokode[19]. Instead of using the curved imaging device, we use a optical mask and a light source to form a beacon, and the relative rotation angle of the camera is determined precisely with ID information.

4.1. Evaluation of image quality by simulation

As described at Section 2.2, images on the sensor formed by each ommatidium are well registered if the angle between two GRIN lenses is sufficiently small. In this section, we show the effect of the registration error to the image quality by simulation. While the curvature of the image surface also causes defocus, in practice it is negligible because the thickness of each lens is very small. We also simulate the radiometric distribution (vignetting) of GRIN lens [18]. Figure 3 shows the images with different angle between the GRIN lenses. A denser array of ommatidia makes the image better, because the well-aligned portion of the images are dominant. Adequate limit of field of view is also very effective to improve the image quality as shown in the bottom picture, which simulates an angle limiter such as a parallax barrier.

4.2. Angular Position Measurement

We use a Krill-eye optical system for the case of $M = 0$ (focused at infinity). Instead of curved imaging sensor, we make a beacon with an optical mask at the focused surface and a light source. The light through each point on the mask results in a pencil of parallel rays as shown in Figure 9(a). The virtual image of the mask seen from the outside the Krill-eye Beacon is at infinity. The light is observed by a camera focused at infinity, and the pattern of the mask is always focused on the camera's sensor. Since the ray parallel to the optical axis of the camera is always focused at the center of the sensor, we can determine the relative angle by decoding the image captured by the camera. Translating the camera does not affect to the estimation of the rotation angle, and the mask pattern is always in focus with the camera focused at infinity. Since we have a finite diameter of the
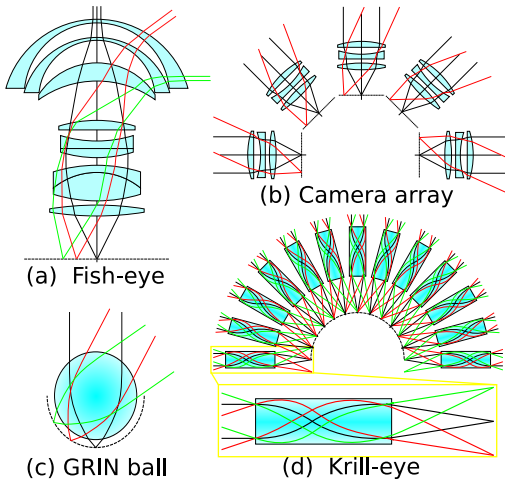

Figure 8. Four alternatives for wide-angle optical system. (a) Fisheye-lens : The most common lens design for wide-angle cameras, (b) Camera array : To cover whole angle of view, multiple cameras are arranged and registered precisely. (c) GRIN ball : Spherical glass ball lenses are used for laser coupling, but a gradient index lens necessary to compensate for spherical aberration is hard to construct. (d) Krill-eye : Similar to (b) but the image is not inverted to form a superposed single image shared by all lenses.
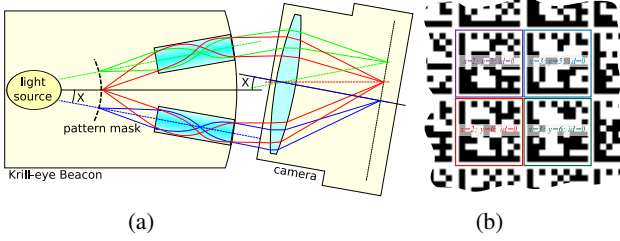
Figure 9. Principle of relative rotation estimation using a Krill-eye Beacon and camera. (a) The code observed at the center of the image in the camera is related to the location on the mask where the direction is same to the optical axis of the camera. Translation of the camera does not affect to the estimation of the rotation angle. The mask pattern is always in focus since the camera is focused at infinity. (b) A tiled matrix of Data Matrix codes encode identification and angular information. Each 10×10 symbol stores its physical position in the Data Matrix pattern, and a single byte of identification information repeated across each Data Matrix.

lens on the camera, some area on the mask is seen in the circle of confusion which is used to decode the angle.

4.2.1 Prototype of Krill-eye Beacon

We present a prototype of a Krill-eye Beacon as shown in Figure 10. We use 9 optical elements with $20°$ rotation each, so they collectively cover approximately $180°$. The GRIN lenses have a diameter of $1.8mm$, and effective length of $9.63mm (= 0.52P)$. We used two GRIN lenses of length $4.26mm (= 0.23P)$ and $5.37mm (= 0.29P)$, positioned end to end with no gap. The constants of the lens are $n_0 = 1.608$ and $\sqrt{A} = 0.339$, therefore, the focal length is $-14.96mm$. The transparency mask is printed by Heidelberg Herkules imagesetter, and we used a red LED as the light source as shown in Figure 11.

For the mask design, we used tiled Data Matrix codes[14]. As shown in Figure 9(b), we use a tiled array of 10×10 Data Matrix codes with one row/column of silent cells between adjacent codes. The 10×10 array encodes 3 bytes of data, and another 5 bytes of Reed-Solomon error correcting code. We allocate one byte to the ID that is repeated across all the Data Matrix codes, and one byte each for the x and y positions of the Data Matrix. This allows the camera to directly read out the relative position and ID of the viewable Data Matrix code from the captured photo.

Additionally, the displacement of each visible Data Matrix from the center of the image gives a better estimate of the angular position of the camera using code interpolation. We compute the fractional position (x_f, y_f) of the center of taken image (p_c) using the coordinates of four corners of the Data Matrix $p_n (n = 0 \cdots 3)$,

$$\begin{pmatrix} x_f \\ y_f \end{pmatrix} = \begin{pmatrix} v_x & v_y \end{pmatrix}^{-1} v_d + \begin{pmatrix} x \\ y \end{pmatrix},$$

where $v_x = p_1 - p_0$, $v_y = p_0 - p_3$ and $v_d = p_c - (p_0 + p_1 + p_2 + p_3)/4$. We use the average of the fractional codes if multiple Data Matrix codes are observed. Unlike most other fiducial based pose estimation techniques, the camera directly reads out the digital angular information, and does not have to estimate the angle based on the local shape of the fiducial.

4.2.2 Estimation of the angle

We confirmed the performance of relative rotation angle estimation using our prototype. Figure 12(a) shows the result of extracted Data Matrix codes, and the estimated angle of rotation is shown in Figure 12(b). Since two lenses out of nine are not aligned well, we see some errors at the areas of $20° - 40°$ and $80° - 100°$. Standard deviation of angle estimation is 2.17deg.
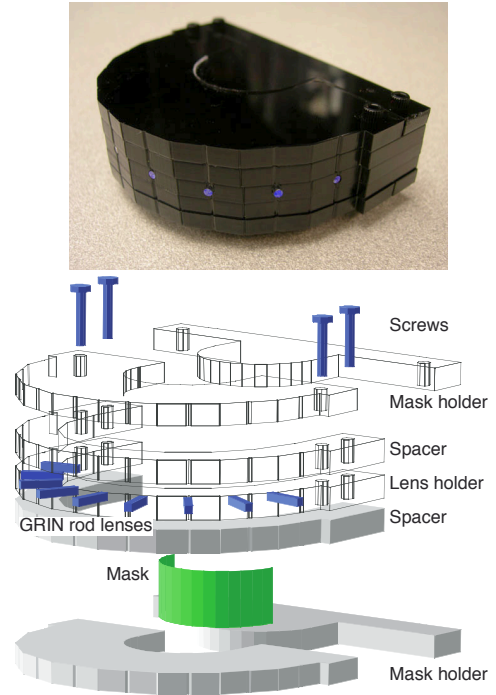

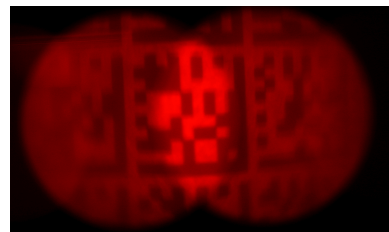Figure 10. Prototype of Krill-eye Beacon with nine GRIN lenses.

Figure 11. One of the image captured by a camera placed outside the Krill-eye Beacon.
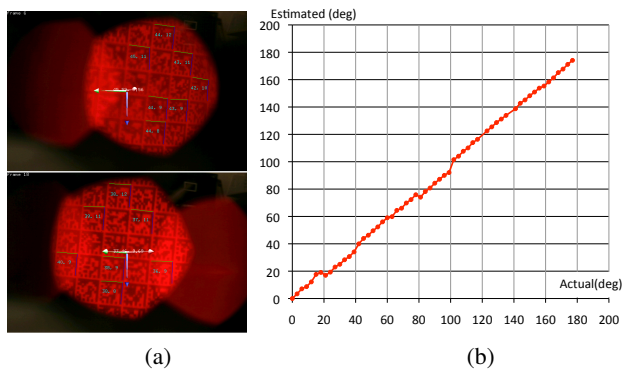
Figure 12. (a) The identified DataMatrix codes. See supplemental materials for all frames over $180°$ rotation. (b) Evaluation of angle estimation using Krill-eye Beacon.

5. Future work and discussion

While we have applied the Krill-eye optics for rotation angle estimation, evaluations of the image quality taken with a dense array of GRIN lenses is worth doing to show the ability for the wide angle cameras. The manufacturing method to precisely align the GRIN lenses is also important.

We propose a novel optical arrangement for wide angle imaging system, named "Krill-eye", inspired by compound eyes of animals. It consist of GRIN lenses aligned on a spherical surface, and it produces distortion-free, uniform image quality under angular variation. We show two constraints to be satisfied simultaneously to form a focused image with several lens elements, and derive a continuous relationships from 1:1 flat imaging systems of scanners to the vision of animals focused at infinity. We preliminary confirm the image quality with a prototype of the proposed optics. We also show a practical application with proposed optics as a beacon to measure the relative rotation angle between the light source and the camera.

References

[1] Dawes' limit. http://en.wikipedia.org/wiki/Dawes'_limit.

[2] Lobster eye x-ray imaging system and method of fabrication thereof. *US Patent 7231017*, 2007.

[3] J. W. Duparré and F. C. Wippermann. Micro-optical artificial compound eyes. *Bioinspiration & Biomimetics*, 1(1):R1–R16, 2006.

[4] C. H.-S. et al. Imaging properties of the gabor superlens. *J. Opt. A: Pure Appl. Opt.*, 1:94–102, 1999.

[5] G. W. F. et al. Lobster-iss: an imaging x-ray all-sky monitor for the international space station. volume 4497, pages 115–126. SPIE, 2002.

[6] J. D. et al. Artificial apposition compound eye fabricated by micro-optics technology. *Appl. Opt.*, 43(22):4303–4310, 2004.

[7] J. T. et al. Thin observation module by bound optics (tombo): Concept and experimental verification. *Appl. Opt.*, 40(11):1806–1813, 2001.

[8] R. D. et al. Curving monolithic silicon for nonplanar focal plane array applications. *Appl. Phys. Letters*, 92(9):091114, 2008.

[9] D. Gabor. *UK Patent 541753*, 1940.

[10] T. Georgiev. On the brightness in images captured with conventional and compound eye cameras. *Adobe Tech. Report*.

[11] J. Gluckman and S. K. Nayar. Ego-motion and omnidirectional cameras. In *ICCV '98: Proceedings of the Sixth International Conference on Computer Vision*, page 999, Washington, DC, USA, 1998. IEEE Computer Society.

[12] T. P. Grayson. Curved focal plane wide-field-of-view telescope design. volume 4849, pages 269–274. SPIE, 2002.

[13] R. A. Hicks and R. K. Perline. Equiresolution catadioptric sensors. *Applied Optics*, 44(29):6108–6114, 2005.

[14] ISO. Automatic identification and data capture techniques – Data Matrix bar code symbology specification. ISO/IEC 16022:2006, 2006.

[15] R. Kingslake. *A History of the Photographic Lens*. Academic Press, 1989.

[16] Y. Koike, Y. Sumi, and Y. Ohtsuka. Spherical gradient-index sphere lens. *Applied Optics*, 25:3356–3363, 1986.

[17] M. F. Land and D.-E. Nilsson. Animal eyes. *Oxford unifersity press*, 2002.

[18] K. Matsuhita and M. Toyama. Unevenness of illuminance caused by gradient-index fiber arrays. *Applied Optics*, 19:1070–1075, 1980.

[19] A. Mohan, G. Woo, S. Hiura, Q. Smithwick, and R. Raskar. Bokode: Imperceptible visual tags for camera based interaction from a distance. *proc. SIGGRAPH*, 2009.

[20] H. Nagahara, Y. Yagi, and M. Yachida. Wide field of view head mounted display for tele-presence with an omnidirectional image sensor. *CVPR Workshop*, 7:86–86, June 2003.

[21] H. Naghara, K. Yoshida, and M. Yachida. An omnidirectional vision sensor with single view and constant resolution. *proc. ICCV*, pages 1–8, 2007.

[22] S. Okura, R. Kawakami, and K. Ikeuchi. Simple surface reflectance estimation of diffuse outdoor object using spherical images. *ACCV'07 Workshop on Multi-dimensional and Multi-view Processing*, 2007.

[23] A. G. Peele, K. A. Nugent, A. V. Rode, K. Gabel, M. C. Richardson, R. Strack, and W. Siegmund. X-ray focusing with lobster-eye optics: a comparison of theory with experiment. *Appl. Opt.*, 35(22):4420–4425, 1996.

[24] J. D. Rees. Non-gaussian imaging properties of grin fiber lens arrays. *Appl. Opt.*, 21(6):1009–1012, 1982.

[25] T. Svoboda, T. Pajdla, and V. Hlavac. Epipolar geometry for panoramic cameras. *proc. ECCV*, page 218, 1998.

[26] P. Swain and D. Mark. Curved ccd detector devices and arrays for multispectral astrophysical applications and terrestrial stereo panoramic cameras. volume 5499, pages 281–301. SPIE, 2004.

[27] K. Yamazawa, Y. Yagi, and M. Yachida. Omnidirectional imaging with hyperboloidal projection. *Proc. Int. Conf. on Intelligent Robots and Systems*, 2:1029–1034, 1993.